Numerical simulations of traffic data on networks via fluid dynamic approach ⋆

G. Bretti [a], A. Cutolo [b], B. Piccoli [c]

[a] *Me.Mo.Mat Department of University "La Sapienza", Via A. Scarpa 16, 00161 - Rome, Italy*

[b] *Diima Department of the University of Salerno, Via Ponte Don Melillo, 84084 - Fisciano(Sa), Italy*

[c] *Istituto per le Applicazioni del Calcolo "M. Picone", Viale del Policlinico 137, 00161 - Rome, Italy*

Abstract

In this paper we introduce a simulation algorithm based on a fluid-dynamic model to reproduce the behavior of traffic in a portion of the urban network in Rome. Numerical results, obtained comparing experimental data with numerical solutions, show the effectiveness of our approximation.

Key words: scalar conservation laws, 65M06, traffic flow, 90B20, fluid-dynamic models, 90B10, finite difference schemes, 35L65, boundary conditions, 34B45.

⋆ The authors would like to thank Roberto Natalini for the interesting discussions and suggestments

Email addresses: g.bretti@iac.cnr.it (G. Bretti), a.cutolo@diima.unisa.it (A. Cutolo), b.piccoli@iac.cnr.it (B. Piccoli).

1 Introduction

In this paper we develop an algorithm to determine the evolution in time of traffic quantities, such as flux, density and cars' speed, on single roads and on networks. We focus on a portion of the urban area in Rome usually subject to congestion, namely Viale del Muro Torto, for which measured traffic data are available. We consider the LWR model with Daganzo-Newell flux and our work consists in the calibration of system parameters in such a way to give a good reconstruction of traffic behavior. The numerical scheme used is the Godunov scheme and it was first proposed in [3]-[4] for road networks. The basic idea is to compute approximate flux and density on a single road, assuming as boundary conditions traffic data measured at the endpoints of it. An estimate of the validity of this procedure is obtained by comparing solutions produced numerically and experimental data detected on the road. Measured data are provided by the municipal society for traffic monitoring and control of Rome, namely ATAC S.p.A. Traffic is observed through an Intelligent Transport System technology, where each subsystem in it, represented by a sensor placed along roads of the city, acquires every minute ($\Delta\tilde{t} = 1$ is the sensor time unit) traffic data such as the flux $\tilde{f}$, the velocity $\tilde{v}$ and the occupation rate $\tilde{o}$. Since each sensor generates a magnetic field, the flux is intended as the number of cars crossing it per minute, the velocity is the average speed of cars at every minute, while the occupation rate is given by the time passed by cars on a sensor, hence it is the time interval in which cars pass through the magnetic field.

The theory is based on the LWR model applied to networks and was developed in [6]-[7]-[10], see also [16]-[9]-[13]-[14]. The network models of transportation systems are assumed to be static in classical approaches, but these models do not allow a correct simulation of heavily congested urban road networks. For this reason, traffic engineers have been studying dynamic traffic assignment or *within-day* models, thus rendering necessary the use of traffic simulation mod-

els. Such models, principally created from static network traffic assignments, can be divided in microscopic, mesoscopic and macroscopic (see [1] and the references therein). The main problems of the static approach are that it does not properly reproduce the backward propagation of shocks and the difficulty of collecting experimental data to test the validity of the models. Many other ideas have been developed by researchers studying traffic from other perspectives, see for instance [8]-[15]-[10].

In the 1950s James Lighthill and Gerald Whitham, two experts in fluid-dynamics, and independently P. Richards, [17]-[18], thought that the equations describing the flow of water could also describe the flow of car traffic. Fluid-dynamic models for traffic flow seem the most appropriate to detect some phenomena as shocks formation and propagation on roads, since solutions can develop discontinuities in a finite time even starting from smooth initial data (see [2]). This nonlinear formulation, based on the conservation of cars, is given by:

$$\partial_t \rho + \partial_x f(\rho) = 0, \tag{1.1}$$

where $\rho = \rho(t, x)$ is the car density, with $\rho \in [0, \rho_{max}]$, $(t, x) \in \mathbf{R}^2$ and ρ_{max} is the maximum car density. The flux $f(\rho)$ is given by ρv, where v is the average velocity of cars. Assuming v to be a smooth decreasing function of the density ρ, also f depends only on ρ and its graph is called the *fundamental diagram*. We always further assume that f, as function of ρ, is concave.

In more detail, the procedure followed in our simulations consists of the steps:

0. data capturing;
1. data cleaning;
2. calibration of flux parameters;
3. generation of approximate solution;
4. computation of errors.

The main results achieved with the mentioned algorithm are:

- the calibration of traffic parameter, providing the maximum velocity v_{max} very close to measured one $\tilde{v}_{max}$;
- the description of traffic behavior, namely of flux and density, with a good approximation.

Focusing on the latter, the percentage error is 11% in the free phase and 19% in the congested phase of traffic. Note that in the congested phase the percentage error is comparable to error detected by sensors, which is around 20%.
Another important byproduct is the reconstruction of the traffic datas on the whole network. In particular, this permits to reconstruct the queues evolutions thus permitting a good estimates of the travelling times.

The papers is organized as follows: Section 2 is devoted to the description of the mathematical model, while the approximation algorithm is presented in Section 3. In Section 4 the results obtained for the roads composing the network are showed and a comparison between numerical and measured solutions is established. Some animations are reported on the web page [5].

2 LWR on networks

A general road network is defined as a finite number of one-way roads modeled by intervals $[a_i, b_i]$ that meet at some junctions. In order to describe the evolution in time of traffic we use the LWR model and describe the dynamics at junctions. A Riemann problem for a scalar conservation law is a Cauchy problem for an initial data of Heaviside type, that is piecewise constant with only one discontinuity. Once Riemann problems are solved, a solution to Cauchy problems can be obtained by wave front tracking, see [2]. Since the flux is concave, the Riemann solutions are of two types: continuous waves called rarefactions and traveling discontinuities called shocks. For a junction, a Rie-

mann problem is a Cauchy problem with an initial data that is constant on each road. Junctions play a fundamental role, as the system at a junction is under-determined, even after prescribing the conservation of cars. Due to finite speed of waves in solutions to (1.1), it is enough assign the dynamics at each junction separately to obtain an evolution on the whole network.
In order to show the main difficulties arising in the dynamics definition, we focus on a simple junction with one incoming and one outgoing road and in particular, we fix the case where the incoming road is occupied by cars with maximum density, while the outgoing road is empty, see Figure 1.

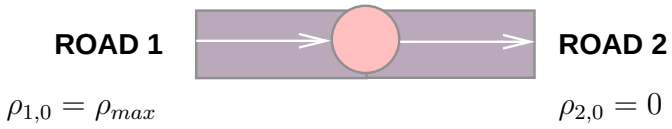

Fig. 1. A particular situation in a junction with one incoming and one outgoing road.

Let us denote the initial datum on road i by $\rho_{i,0}$, $i = 1, 2$, then:

$$\rho_{1,0}(x) = \rho_{max}, \quad \rho_{2,0}(x) = 0. \tag{2.2}$$

Two possible extreme behaviors of cars are expected, namely: all cars flow towards the outgoing road (entropy solution) or all cars do not pass through the junction (non-entropy solution). In this way two different solutions ρ and $\tilde{\rho}$ on the network are determined. Namely:

$$\rho_1(t,x) = \begin{cases} \rho_{max}, & \text{if } x < f'(\rho_{max})t \\ (f')^{-1}\left(\frac{x}{t}\right), & \text{if } f'(\rho_{max})t < x < 0, \end{cases}$$

$$\rho_2(t,x) = \begin{cases} (f')^{-1}\left(\frac{x}{t}\right), & \text{if } 0 \leq x < f'(0)t, \\ 0, & \text{if } x > f'(0)t, \end{cases}$$

while $\tilde{\rho}_1 = \rho_{1,0}$, $\tilde{\rho}_{2,0} = \rho_2$.

Hence, the conservation of cars quantity through the junction, which reads as:

$$\sum_{\text{incoming roads}} \text{incoming fluxes} = \sum_{\text{outgoing roads}} \text{outgoing fluxes},$$

holds for both solutions: in other words the solely conservation of cars is not sufficient to ensure uniqueness. Therefore, a map assigning solutions to initial data, called a Riemann solver at junctions, is needed. A classification of possible choices for Riemann solvers, in the above case, have been recently presented in [11].

For a general junction with n incoming and m outgoing roads, various authors ([7,8,14,16]) used Riemann solvers associated to the following rule:

(A) there exists a traffic distribution matrix $A = \{\alpha_{j,i}\}$ of coefficients $0 \leq \alpha_{j,i} \leq 1$ giving the percentage of cars flowing from the i-th incoming road to the j-th outgoing one and

$$\sum_{j=n+1}^{n+m} \alpha_{j,i} = 1, \text{ for every } i \in \{1, \dots, n\}. \tag{2.3}$$

First notice that rule (A) implies the conservation of cars through the junction. In fact, if f_i and f^j are, respectively, the fluxes on the i-th incoming road and on the j-th outgoing one, from (2.3) we have:

$$\sum_j f^j = \sum_j \sum_i \alpha_{j,i} f_i = \sum_i \sum_j \alpha_{j,i} f_i = \sum_i f_i.$$

One may expect that rule (A) is sufficient to describe in a unique fashion the dynamics at junctions, but it is not the case.

Consider again a junction with one incoming and one outgoing roads and the initial data (2.2). Both solutions ρ and $\tilde{\rho}$ satisfy rule (A).

To maximize the entropy flux, as for conservation laws, see [2], we fix another

rule:

(B) The number of cars passing the junction is the maximum possible (respecting rule (A)).

In case $m \geq n$ (and under some generic assumption), rules (A) and (B) ensure uniqueness of solutions on networks. Moreover, for a single incoming road, it is easy to check that rule (B) is equivalent to maximize the average velocity. We recall briefly the procedure for constructing solutions, for further details see [7]. We use initial data ρ_{i0} on incoming roads (ρ_{j0} on outgoing roads) at the endpoints interacting with junctions and we determine the new states, called $\hat{\rho}_i$ ($\hat{\rho}_j$ on outgoing roads), in such a way that waves emerge out of junctions. Since this rule leads to a constraint on waves speed (negative on incoming roads, positive on outgoing roads), it defines a region Ω where we obtain maximized incoming fluxes $\hat{\gamma}_i$ for $i \in \{1, ..., n\}$, as prescribed by rule (B). Let $\tau : [0,1] \mapsto [0,1], \tau(\sigma) = \sigma$, be the well-defined map satisfying the following

$$\tau(\rho) \neq \rho, \qquad f(\tau(\rho)) = f(\rho),$$

for each $\rho \neq \sigma$. The new states $\hat{\rho}_i$ are uniquely determined from $\hat{\gamma}_i$ by inverting the relation:

$$f(\hat{\rho}_i) = \hat{\gamma}_i, \qquad \text{with } \hat{\rho}_i \in \begin{cases} \{\rho_{i,0}\} \cup]\tau(\rho_{i,0}), 1], & \text{if } 0 \leq \rho_{i,0} \leq \sigma, \\ [\sigma, 1], & \text{if } \sigma \leq \rho_{i,0} \leq 1. \end{cases} \tag{2.4}$$

Recalling rule (A), maximized outgoing fluxes $\hat{\gamma}_j \doteq \sum_{i=1}^{n} \alpha_{ji} \hat{\gamma}_i, j = n+1, ..., n+m$, are derived and the new states $\hat{\rho}_j$ are computed analogously.
The weak solution on each road is given by the solution to Riemann problem with data $(\rho_{i0}, \hat{\rho}_i)$ for incoming roads and $(\hat{\rho}_j, \rho_{j0})$ for outgoing roads and it can be, respectively, a shock or a rarefaction.

As the speed of propagation is finite, following [7] we can build a sequence of solutions to Cauchy problems via a wave front tracking algorithm.
From now on we set $\rho_{max} = 1$ and the flux function $f = v\rho$ is assumed to be:

$$f(\rho) = \begin{cases} \frac{f_{max}}{\sigma}\rho & \text{if } 0 \leq \rho \leq \sigma, \\ f_{max}\left(\frac{\rho_{max}-\rho}{\rho_{max}-\sigma}\right) & \text{if } \sigma \leq \rho \leq \rho_{max}, \end{cases} \tag{2.5}$$

where σ is the value of density corresponding to the maximum flux f_{max}, see Fig. 2. Such fundamental diagram is usually called Daganzo-Newell flux

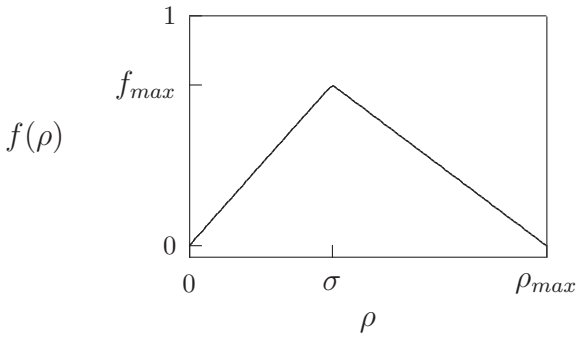

Fig. 2. The flux function.

function. Modelization of the congested phase is complicated, since in this case the flux assumes a scattering behavior, therefore there are many possible choices for flux function. Our approach is to use a simple model with reasonable properties:

1) there are only two characteristic velocities;
2) it is able to reproduce empirical phenomena of backward moving clusters.

3 Description of the approximation algorithm

Our procedure is composed by the following steps:

0. data capturing;

1. data cleaning;
2. calibration of flux parameters;
3. generation of approximate solution;
4. computation of errors.

Let us give the details.

3.0.1 Step 0: data capturing

Traffic is observed by sensors located along roads. Sensors acquire traffic data, i.e. the flux, the velocity and the occupation rate, along each road with a frequency of one minute within an entire day. In the portion of network we are considering, namely Viale del Muro Torto, described in Section 4, there are 7 sensors per direction.

3.0.2 Step 1: data cleaning

For each segment, traffic measured data represented by the flux, namely the number of cars crossing it per minute, the velocity, considered as the average speed of cars at every minute, and the occupation rate, namely the time interval in which cars exit the magnetic field generated by sensors, are stored in a file named as the code of the road itself. Due to their structure, such files cannot be used directly by simulation algorithm, hence we need to apply a standardization procedure to consent data loading to the program.
Since density is not detected by sensors, we may recover its value on each road as the ratio between measured flux $\tilde{f}^i$ and velocity $\tilde{v}^i$:

$$\tilde{\rho}^i = \frac{\tilde{f}^i}{\tilde{v}^i}, \text{ if } \tilde{v}^i \neq 0, \text{ for } i = 1, \dots, T,$$

with T the final observation time expressed in minutes. Otherwise, if $\tilde{v}^i = 0$, a selection and cleaning of measured data is done. More precisely, traffic data are

required to verify the following admissibility conditions. When the velocity is null a flux different from zero cannot be assumed, hence in this case we exclude such values. If the flux is null and the occupation rate is also null then the density is taken equal to zero, otherwise we can assume the density to be maximal, as displayed in (3.6):

$$\text{if } \tilde{v}^i = 0 \text{ and } \tilde{f}^i = 0 \Rightarrow \begin{cases} \text{if } \tilde{o}^i = 0 \Rightarrow \tilde{\rho}^i = 0, \\ \text{if } \tilde{o}^i \neq 0 \Rightarrow \tilde{\rho}^i = \rho_{max}. \end{cases} \tag{3.6}$$

Since the most complete data sets are from sensors on road segments 544, 549 and 548, we mainly focused on them and, in this case, the percentage of excluded data is around 5.6%.

3.0.3 Step 2: calibration of flux parameters

A calibration procedure is applied to each segment of road network. It consists of a minimization with two parameters, namely f_{max} and σ, to determine the analytical expression of flux function (2.5), where the maximum density ρ_{max} can be theorical, and in this case it is fixed to 333 on the whole network, or measured and eventually different on each road. The optimized parameters are computed in the original scale and the maximal speed is consequently derived as $v_{max} = f_{max}/\sigma$. Flux parameters obtained by the calibration procedure determine different flux functions on each road, thus adapting its shape to their different features.

To measure calibration errors we consider the functional J, given by the sum of squares of differences between analytical and measured fluxes. Separating

into free and congested phase, we get:

$$J = \begin{cases} J_{free} = \sum_{\tilde{\rho}^i \leq \sigma} \left(\frac{f_{max}}{\sigma} \tilde{\rho}^i - \tilde{f}^i \right)^2, \\ J_{congested} = \sum_{\tilde{\rho}^i > \sigma} \left(f_{max} \left(\frac{\rho_{max} - \tilde{\rho}^i}{\rho_{max} - \sigma} \right) - \tilde{f}^i \right)^2. \end{cases} \tag{3.7}$$

3.0.4 Step 3: generation of approximate solution

We produce approximate solutions on the network solving problem (1.1) on each road. To this aim we make a space-time discretization introducing a *numerical grid* in $\mathbf{R}^N \times (0, T)$, where:

- Δx is the space grid size;
- Δt is the time grid size;
- $(t_l, x_m) = (l\Delta t, m\Delta x)$, for l, m varying, respectively on a subset of $\mathbf{N}$ and $\mathbf{Z}$, are the grid points.

For a function v defined on the grid we write $v_m^l = v(t_l, x_m)$ for $l = 0, \ldots, N$ and $m = 0, \ldots, M$, with N the number of iterations in time and M the number of space steps. We also use the notation ρ_m^l for $\rho(t_l, x_m)$ when ρ is the density on the (t, x) plane. In order to show the approximation procedure, let us focus on a single segment within the network. Our aim is to reconstruct the evolution of flux and density in the considered segment by applying the algorithm based on Godunov scheme and presented in [3].
Let us now briefly describe the algorithm. The initial datum is approximated by a piecewise constant function; then the corresponding Riemann problems are solved exactly and a global solution is simply obtained by piecing them together; finally, one takes the mean and proceeds by induction.

We take a piecewise constant approximation of the initial datum:

$$v_m^0 = \frac{1}{\Delta x} \int_{x_m}^{x_{m+1}} u_0(x)dx, \quad m \geq 0 \tag{3.8}$$

and the scheme defines v_m^l recursively starting from v_m^0. Solutions to Riemann problems from $x_{m-1/2}$ are taken and then projected on a piecewise constant function by

$$v_m^{l+1} = \frac{1}{\Delta x} \int_{x_{m-1/2}}^{x_{m+1/2}} v^{\Delta}(t_{l+1}, x)dx \tag{3.9}$$

and v^{l+1} is computed by the Gauss-Green formula. Under the CFL condition

$$\Delta t \sup_{m,l} \Big\{ \sup_{u \in I(u_m^l - 1/2, u_{m+1/2}^l)} |f'(u)| \Big\} \leq \Delta x, \tag{3.10}$$

the waves, generated by Riemann solutions, do not influence the solution in $x = x_{m+1/2}$, for $t \in (t_l, t_{l+1})$. As the flux is time invariant and continuous, we can put it out of the integral and set $g^G(u, v) = f(W_R(0; u, v))$, with $W_R\left(\frac{x}{t}; v_-, v_+\right)$ the self-similar solution between v_- and v_+. Under the condition (3.10), the scheme can be written as:

$$v_m^{l+1} = v_m^l - \frac{\Delta t}{\Delta x}(g^G(v_m^l, v_{m+1}^l) - g^G(v_{m-1}^l, v_m^l)). \tag{3.11}$$

The expression of the numerical flux for Godunov method is given by

$$g^G(u, w) = \begin{cases} \min_{z \in [u,w]} f(z) & \text{if } \ u \leq w, \\ \\ \max_{z \in [w,u]} f(z) & \text{if } \ w \leq u. \end{cases}$$

Boundary conditions are imposed as follows. At the incoming boundary we set $u(a, t) = \rho_1(t), \ t > 0$. We practically proceed by inserting a ghost cell and

defining the approximate solution at node x_0 as:

$$v_0^{l+1} = v_0^l - \frac{\Delta t}{\Delta x}(g^G(v_0^l, v_1^l) - g^G(u_1^l, v_0^l)), \tag{3.12}$$

where $u_1^l(t) = \frac{1}{\Delta t}\int_{t_l}^{t_{l+1}} \rho_1(t)dt$ takes the place of v_{-1}^l. An outgoing boundary can be treated analogously. Let the final endpoint of a road be $x_N = b$. Then the approximate density expresses as:

$$v_N^{l+1} = v_N^l - \frac{\Delta t}{\Delta x}(g^G(v_N^l, u_2^l) - g^G(v_{N-1}^l, v_N^l)), \tag{3.13}$$

where $u_2^l(t) = \frac{1}{\Delta t}\int_{t_l}^{t_{l+1}} \rho_2(t)dt$ takes the place of v_{N+1}^l, that is a ghost cell value. Input data of the algorithm provided by previous steps of the procedure are:

1. the optimized parameters f_{max}, σ and, eventually, ρ_{max} (if the maximal density is not fixed), to be inserted in the analytical expression (2.5);
2. initial and boundary conditions.

Since the simulation starts during night, we assume an empty configuration of density and, as boundary conditions, we use measured values of density detected by sensors located in the initial and final endpoints of the segment, see Fig. 3. The simulation algorithm produces numerical values of flux and density along the entire road, therefore we can derive the flux, denoted by $f^{num,l}$, computed at a certain time t_l in the point of the road corresponding to the sensor position.

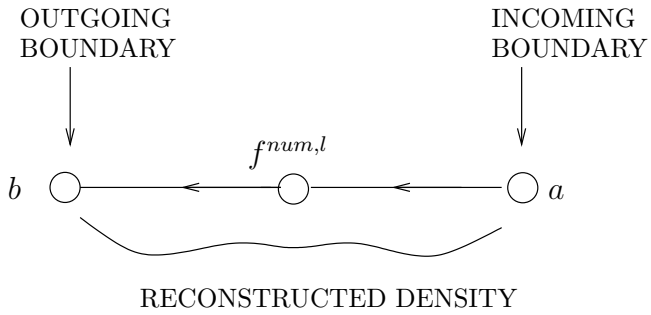

Fig. 3. Schematization of the approximation procedure on a segment at time t_l.

3.0.5 Step 4: computation of errors

Let us introduce the approximation error. To this aim we define $\tilde{f}_{max}$ as the minimal flux value such that 90% of measured fluxes are below it and, at each time step, we compute errors as the differences between numerical flux f^{num} and measured flux $\tilde{f}$:

$$E = \begin{cases} E_{free} = \sum_{k_1 \in K_{free}} |f^{num,k_1} - \tilde{f}^{k_1}| / \tilde{f}_{max}, \\ E_{cong} = \sum_{k_2 \in K_{cong}} |f^{num,k_2} - \tilde{f}^{k_2}| / \tilde{f}_{max}, \end{cases} \tag{3.14}$$

where K_{free} and K_{cong} are, respectively, the sets of effective indexes of admissible values of densities in free and in congested part, obtained excluding densities corresponding to non-admissible fluxes. In particular, we are interested in the average errors:

$$E_f = E_{free}/\#K_{free}, \quad E_c = E_{cong}/\#K_{cong}.$$

4 Simulation results

Here we report some results obtained by the application of the algorithm described in Section 3.

Input data of simulation algorithm, provided by ATAC S.p.A., refer to an area

of the city of Rome, Viale del Muro Torto, which links the historical center with the northern area of the city. We consider the path covered moving from Corso d'Italia towards Piazza del Popolo and we fix within the network a single segment of length 776 meters, see Fig. 4. Notice that black circles on the map represent sensors.

In the following Fig. 5 we represent a diagram of measured flux during an

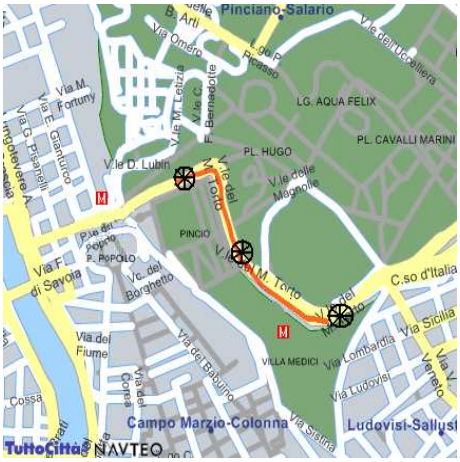

Fig. 4. Viale del Muro Torto.

entire week. The first part of the graph, i.e. up to density $\rho \sim 55$, represents the free phase of traffic, while the second part reproduces the congested phase.

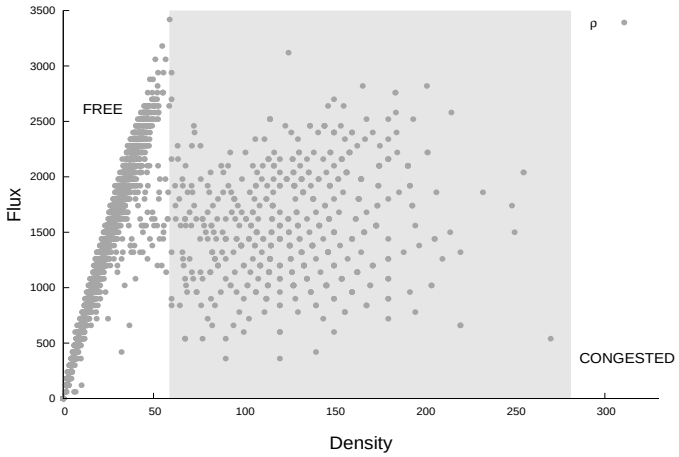

Fig. 5. Measured flux-density diagram.

4.1 Calibration of Fundamental diagrams for road segments

Here we consider all roads composing the network of Viale del Muro Torto. The fitting procedure, characterized by the steps 0)-1)-2) of the algorithm described in Section 3, is performed assuming different initial conditions of flux parameters. A two-parameters constrained optimization is obtained by the following procedure organized in four steps:

i) in the congested phase we apply a least square method (regression line) and we call $\bar{f}^{k_2}$ the values approximating $\tilde{f}^{k_2}$;

ii) setting

$$E_{regr} = \sum_{k_2 \in K_{cong}} (\bar{f}^{k_2} - \tilde{f}^{k_2})$$

the mean square error, we compute the average error:

$$\mu = \frac{E_{regr}}{\#K_{cong}};$$

iii) indicating by δ the variance:

$$\delta = \frac{\sum_{k_2 \in K_{cong}} ((\bar{f}^{k_2} - \tilde{f}^{k_2})^2 - \mu)}{\#K_{cong}}$$

we discard the values of congested flux not satisfying the condition:

$$(\bar{f}^{k_2} - \tilde{f}^{k_2})^2 < \mu + \sqrt{\delta}.$$

iv) taking ρ_{max} as the maximal measured density on each road a constrained optimization on the screening data is operated to determine σ and f_{max}.

Simulations are performed starting from different initial values within the intervals:

$$10 < \sigma < 70, \qquad 1500 < f_{max} < 3450. \tag{4.15}$$

Since the maximum velocity is defined as the ratio f_{max}/σ, we derive v_{max} from the optimized values. Then we compare it to the maximum velocity $\tilde{v}_{max}$

computed as the average of maximum speed measured by sensors in the free phase of traffic.

In Table 1 we report the results of the calibration procedure. From calibration of data produced by sensor located inside the road, we get optimized parameters in the original scale:

$$\sigma = 38.87, \qquad f_{max} = 2258.52, \tag{4.16}$$

hence v_{max} is about 58 km/h. Setting $\Delta x = 77.6$ the examined road is divided into 10 sub-intervals and the CFL condition $\Delta t \; v_{max} < \Delta x$ (reducing all quantities to the same scale, e.g. meters per second) reads:

$$\Delta t \; \frac{58000}{3600} < 77.6 \quad \Leftrightarrow \quad \Delta t < \frac{77.6}{16.11} \quad \Leftrightarrow \quad \Delta t < 4.81.$$

Recalling that $\tilde{\Delta} t$ corresponds to 1 min (60 sec):

$$\frac{\Delta t}{\tilde{\Delta} t} \; < \; \frac{4.81 sec}{60 sec} \sim 0.08.$$

Assuming $\Delta t = \frac{1}{16} = 0.0625$, with time expressed in minutes, the CFL required by Godunov scheme is respected. In order to impose boundary conditions we use traffic data provided by sensors on the right and on the left endpoint of considered segment as, respectively, incoming ρ_b^{inc} (road code 548) and outgoing boundary data ρ_b^{out} (road code 544), see Fig. 6. The number of iterations

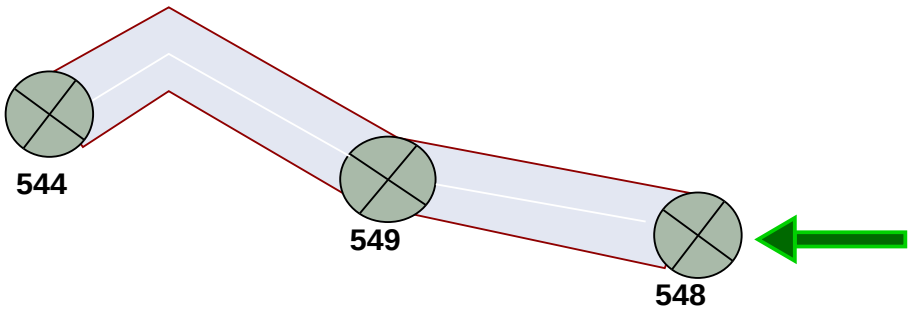

Fig. 6. A road segment in Viale del Muro Torto.

in time of simulation algorithm is $N = 16 \times T$, hence we need to fill the gaps in

		Initial values		Optimized values			
Road code	ρ_{max}	σ	f_{max}	σ	f_{max}	v_{max}	$\tilde{v}_{max}$
544	276	38	2300	37.64705	2063.64395	54.815551	47.35663
544	276	43	2500	38.53337	2110.48027	54.168927	47.35663
544	276	48	2700	37.64705	2060.50058	54.732054	47.35663
548	220	38	2300	45.74509	2451.47698	53.58995	53.00096
548	220	43	2500	45.74497	2451.48191	53.59019	53.00096
548	220	48	2700	45.74507	2451.48745	53.59019	53.00096
549	270	38	2300	38.32250	2227.82598	58.13363	56.82542
549	270	43	2500	39.05808	2313.94563	57.81921	56.82542
549	270	48	2700	38.32198	2227.79486	58.13360	56.82542
556	192	38	2300	26.97233	1919.72807	71.17502	71.17397
556	192	43	2500	26.97230	1919.72505	71.17114	71.17397
556	192	48	2700	25.72385	1763.48061	71.31985	71.17397
600	240	38	2300	54.10050	2847.90330	52.64099	51.70879
600	240	43	2500	54.10109	2847.94053	52.64109	51.70879
600	240	48	2700	53.67810	2791.42491	53.10824	51.70879

Table 1

Two-parameters constrained optimization subject to (4.15) for different initial values with ρ_{max} the maximum density observed on each segment.

the values of densities at the boundaries. This can be done using, for example, a linear interpolating procedure:

$$\rho^{num,l} = \left(1 - \frac{r}{16}\right)\tilde{\rho}_{l_1} + \frac{r}{16}\tilde{\rho}_{l_1+1}, \quad l = 1, \ldots, N,$$

with $l_1 = [l/16]$ and $r = l - l_1$. Average error for free and congested phase are respectively:

$$E_f = 0.1146, \quad E_c = 0.1957.$$

Therefore the percentage error is around 11% for free phase and around 19% for congested phase, thus it is comparable to sensor error which is, in the latter case, around 20%. The following Figures 7, 8, and 9, show a comparison between computed and given fluxes. In the mentioned figures we also report the density values $\tilde{\rho}$, depicted according to the scale on the right side of y-axis. This was done to have an immediate distinction between the two traffic phases, namely free phase and the congested phase, for $\tilde{\rho} > \sigma = 38.87$.

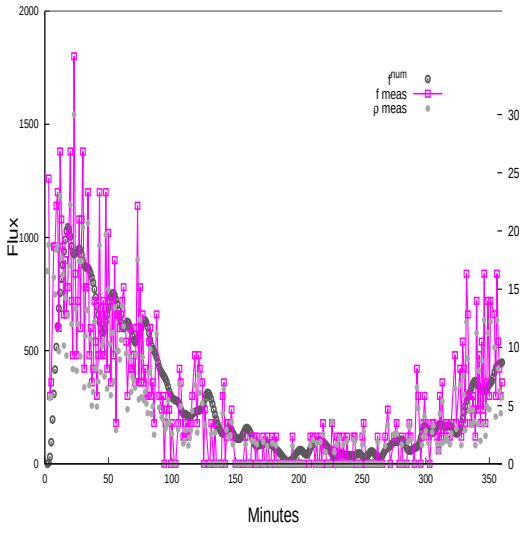

Fig. 7. Comparison between f^{num} and $\tilde{f}$ in the first day, from 0:00 to 6:00 a.m. - free phase only.

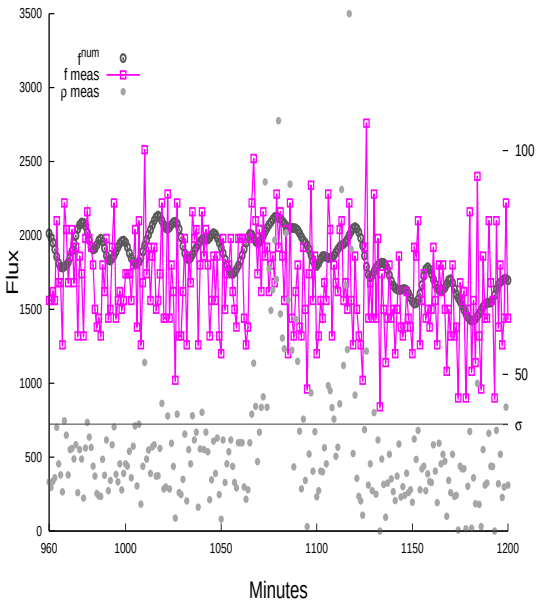

Fig. 8. Comparison between f^{num} and $\tilde{f}$ in the first day, from 16:00 to 20:00.

From the analysis of Figures 7 and 8, it can be noticed that the approximate solution f^{num} seems to substantially follow the profile of the curve of experimental data, except in some zones where the distance between f^{num} and $\tilde{f}$ is quite high. We could consider the curve of approximate solution as a sort of average of the curve given by measured data. In order follow the behavior of our approximation more accurately, in Fig. 8 we restrict to the period 18:00-19:00 and we represent it in Fig. 9.

For sake of completeness we investigated how the frequency with which sensors collect data affect our approximation. To this aim, we applied the optimization procedure supposing that data are provided with a lower frequency, i.e. for a time interval of two minutes and of four minutes. We obtained the following results:

It can be noticed that a lower frequency in collecting data means an inferior quantity of informations: $\tilde{\Delta}t = 2$ corresponds to half of data, $\tilde{\Delta}t = 4$ corresponds to quarter of data. However, from results in Table 4.1, we can observe

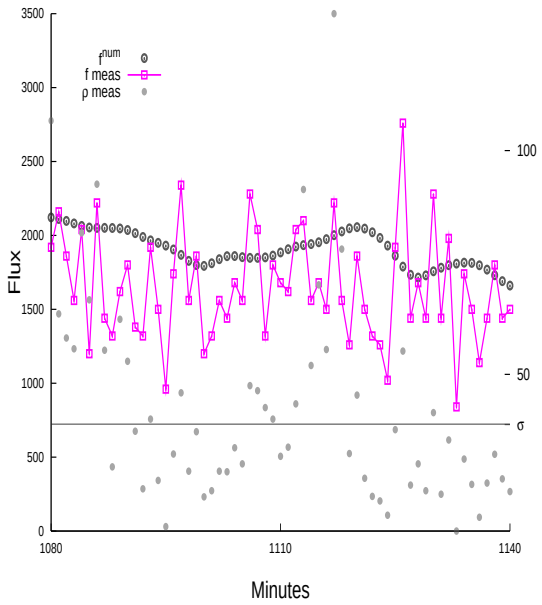

Fig. 9. Comparison between f^{num} and $\tilde{f}$ in the first day, from 18:00 to 19:00.

$\tilde{\Delta}t = 1$		$\tilde{\Delta}t = 2$		$\tilde{\Delta}t = 4$	
E_f	E_c	E_f	E_c	E_f	E_c
0.1146	0.1969	0.1178	0.2025	0.1265	0.2181

Table 2

Two-parameters optimization obtained setting differently the frequency of detecting data by sensors.

a slight worsening in the approximation: the error in the congested case increases less than one percentage point if $\tilde{\Delta}t = 2$ and less than two percentage points if $\tilde{\Delta}t = 4$.

4.2 Data reconstruction

Our algorithm permits to reconstruct the data on the whole road for every time. Some graphs describing the evolution of the density from 6:00 to 10:00 are reported in Fig. 10. An important consequence is the possibility of com-

puting and visualizing the queues forming at the end of the road and moving backwards. Using only the data from sensors, we can only determine if the queue reached one sensor or did not. Since sensors are places every 400 meters (more or less), the average exptected error for the queue length can be of 200 meters. This in turn may give rise to big errors in the estimation of the travelling time (usually communicated to drivers through panels at the entering of the road).

On the contrary our algorithm permits to reconstruct the queue end position at every time, with a low error, thus giving good travelling time estimates.

Related animations are reported on the web page [5].

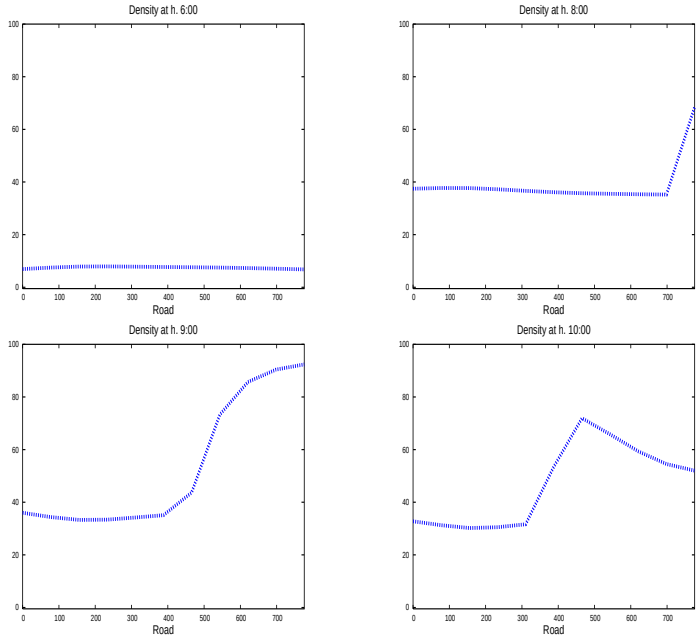

Fig. 10. Reconstruction of the density on the segment between 6:00 and 10:00.

5 Conclusions

Focusing on the comparison between v_{max} and $\tilde{v}_{max}$, we want to point out that the measured velocity values are approached by the approximate velocity values on all roads of the network except on road 544. This is explained by a known inefficiency of the sensor located on road 544.

References

[1] V. Astarita, Node and Link Models for Network Traffic Flow Simulation, *Mathematical and Computer Modelling*, 35 (2002), pp. 643-656.

[2] A. Bressan, *Hyperbolic Systems of Conservation Laws - The One-dimensional Cauchy Problem*, Oxford Univ. Press, 2000.

[3] G. Bretti, R. Natalini and B. Piccoli, *Numerical Approximations of a Traffic Flow Model on Networks*, Networks and Heterogeneous Media, **1** (2006), no. 1, 57-84.

[4] G. Bretti, R. Natalini and B. Piccoli, *Fast Algorithms for the Approximation of a Traffic Flow Model on Networks*, Discrete and Continuous Dynamical Systems - Series B, vol. 6 (2006), pp. 427-448.

[5] G. Bretti and B. Piccoli, http://www.iac.rm.cnr.it/∼bretti/TrafficNumericalSolutions.html .

[6] Y. Chitour and B. Piccoli, *Traffic circles and timing of traffic lights for cars flow*, Discrete and Continuous Dynamical Systems-Series B, **5** (2005), no. 3, 599-630.

[7] G.M. Coclite, M. Garavello and B. Piccoli, *Traffic Flow on a Road Network*, Siam Math. Anal., **36** (2005), no. 6, 1862-1886.

[8] C. F. Daganzo, Fundamental of Transportation and Traffic Operations, Elsevier, New York, (1997).

[9] C. F. Daganzo, *On the variational theory of traffic flow: well-posedness, duality and applications*, Networks and Heterogeneous Media, **1** (2006), no. 4, 601-619.

[10] M. Garavello and B. Piccoli, *Traffic Flow on Networks*, AIMS Series on Applied Mathematics (2006).

[11] M. Garavello, R. Natalini, B. Piccoli and A. Terracina, *Conservation laws with discontinuous flux*, Networks and Heterogeneous Media, **1** (2007), no. 2, 159-179.

[12] B. D. Greenshields, A study in Highway capacity, *Highway Research board Proceedings*, 14 (1935), pp. 448-477.

[13] D. Helbing, S. Lämmer, and J. P. Lebacque, *Self-organized control of irregular or perturbed network traffic*, 239-274 in: C. Deissenberg and R. F. Hartl (eds.) Optimal Control and Dynamic Games, Springer, Dordrecht, 2005.

[14] D. Helbing, J. Siegmeier, and S. Lämmer *Self-organized network flows*, Networks and Heterogeneous Media, vol.2 (2007),pp. 193-210 .

[15] R. Herman and I. Prigogine, *A two-fluid approach to town traffic*, Science, 204 **4389** (1979), 148-151.

[16] J. P. Lebacque, M. M. Khoshyaran, *Modelling vehicular traffic flow on networks using macroscopic models*, in Finite volumes for complex applications II, pp. 551–558, Hermes Sci. Publ., Paris, 1999.

[17] M. J. Lighthill and G. B. Whitham, *On kinetic waves. II. Theory of Traffic Flows on Long Crowded Roads*, Proc. Roy. Soc. London Ser. A, **229** (1955), 317-345.

[18] P. I. Richards, *Shock Waves on the Highway*, Oper. Res., **4** (1956), 42-51.